Archives of Mechanics • Archiwum Mechaniki Stosowanej • 30, 4–5, pp. 663–674, Warszawa 1978

Supersonic flow around flattened bodies and sharp tip wings

G. P. VOSKRESENSKY (MOSCOW)

THE AIM of this paper is to describe some results of the numerical investigation of the supersonic inviscid flow around sharp-nosed, flattened bodies with a bow shock attached to the nose-cone of the bodies and around sharp tip wings with the shock wave attached to the leading edge. The numerical investigation is based on a finite-difference second-order method. The following flow fields have been investigated: around elliptic cones with a large semi-axis ratio $a/b \leqslant 8$ at the angle of attack 10° and $M_\infty = 3.0$; around a non-conical flattened body of the type of delta plane vehicle at the angle of attack 10°: around delta, swept and rhombic-shaped wings with airfoils at the angles of attack 5°, 8° and $M_\infty = 3.0$; 4.0.

Celem pracy jest przedstawienie kilku wyników obliczeń numerycznych dla naddźwiękowego nielepkiego przepływu wokół ostro zakończonych spłaszczonych kadłubów, z falą uderzeniową występującą na stożkowym nosku kadłuba oraz wokół ostrego końca skrzydeł, z falą uderzeniową umiejscowioną na krawędzi natarcia. Obliczenia numeryczne przeprowadzono metodą różnic skończonych, przyjmując aproksymacje drugiego rzędu. Zbadano następujące pola przepływów: wokół stożków eliptycznych przy dużym stosunku półosi $a/b \leqslant 8$ przy kącie natarcia 10° i $M_\infty = 3{,}0$; wokół niestożkowego spłaszczonego kadłuba typu delta przy kącie natarcia równym 10°; wokół delty, skrzydła typu strzały i rombu z powierzchniami nośnymi na kątach natarcia 5°, 8° i $M_\infty = 3{,}0$; 4.0.

Представлены некоторые результаты численного исследования сверхзвукового невязкого обтекания острых сплюснутых тел с ударной волной, присоединенной к вершине, а также остроконечных крыльев с волной, присоединенной к передней кромке. Исследование проводилось с помощью конечно-разностного метода второго порядка точности. Исследовалось течение около эллиптических конусов с большим отношением полуосей $a/b \leqslant 8$ при угле атаки 10° и $M_\infty = 3{,}0$; неконического сильно сплюснутого тела типа дельтаплана при угле атаки 10°, а также около треугольных, стреловидного и ромбовидного профилированных крыльев при углах атаки 5°, 8° и $M_\infty = 3{,}0$; 4,0.

1.

THE DETERMINATION of the aerodynamic characteristics and detailed description of the three-dimensional flow around supersonic vehicles is of great practical importance but at the same time it is mathematically complicated. The best results in this field during the past decade have been achieved with the help of numerical methods.

This paper deals with some numerical results of two problems. The first problem is concerned with the computation of the supersonic flow field around sharp-nosed heavily flattened conical and non-conical bodies, such as a delta plane vehicle with a detached shock wave from the leading edge.

The second problem is concerned with the computation of the supersonic flow around delta, swept or rhombic-shaped sharp tip wings. The wing airfoil may be arbitrary. The shock wave is attached to the leading edge of the wings.

The solution of both problems is based on the numerical method of the computation of three-dimensional supersonic flows developed by K. I. BABENKO and G. P. VOSKRES-

ENSKY in 1961 [1]. This method in application to these problems has been modified. But general features of the method remain the same.

The method is concerned with the problem in some physical domain with initial data and boundary conditions for the system of gasdynamical equations of the stationary inviscid flow. The gas may be chemically-reactive at high temperature.

The flow equations are as follows:

$$\begin{aligned} &\frac{d\bar{V}}{dt} + \frac{1}{\varrho}\,\mathrm{grad}p = 0, \\ &\frac{d\varrho}{dt} + \varrho\,\mathrm{div}\bar{V} = 0, \\ &\frac{d}{dt}\left(\frac{\bar{V}^2}{2} + \frac{\varkappa}{\varkappa-1}\frac{P}{\varrho}\right) = 0. \end{aligned} \tag{1.1}$$

The flow is assumed to be supersonic everywhere with respect to the x-axes and therefore the system (1.1) is x-hyperbolical.

As a result of the chemically-reactive gas, the system equations must be completed at each grid point by the calculation of the velocity of sound and the ratio of specific heats.

The boundary conditions are set on the surface of the body and on the shock wave. The surface of the shock wave is the unknown function and it is determined by the solution process. The initial data surface is set near the vertex of the bodies. The physical domain of the solution is transformed into a simple rectangle by normalizing the distance between the body and the outer shock wave.

The method uses a second-order finite-difference implicit scheme. The solution is marched downstream from the initial data surface $x = x_0$ by the iteration process.

The initial data were obtained by the stationing principle in the case of a sharp nose, because the nose is supposed to be conical with the auto-modelling flow along the coordinate X. The basic algorithm is also used for this purpose.

2.

The first problem is concerned with the supersonic flow field around sharp-nosed flattened bodies, with the bow shock attached to the nose. The algorithm of its numerical solution is described in the paper [2]. The cylindrical coordinates (x, r, φ) are used. The bodies have elliptical cross-sections and their surfaces were governed by the following equation:

$$\begin{aligned} G(x,\varphi) &= a\sqrt{H^2+H_\gamma^2}, \\ H &= \sqrt{Q^2\cos^2\gamma+\sin^2\gamma}, \\ H_\gamma &= dH/d\gamma, \\ Q &= 1/2[1-\mathrm{sign}(\cos\gamma)]Q_u + 1/2[1+\mathrm{sign}(\cos\gamma)]Q_e, \\ \varphi &= \gamma + \mathrm{arctg}(H_\gamma/H), \end{aligned} \tag{2.1}$$

where Q_u and Q_e are the ratio of the semi-axis of the cross-section ellipse (major/minor) for upper and lower parts of the cross-section $a = a(x)$, $Q_u = Q_u(x)$, $Q_e = Q_e(x)$.

The initial data for the conical flows are represented by gas-dynamical functions around a circular cone with the given M_∞ number and the angle of attack equal zero. The angle of the circular cone is equal to the angle of a conical body with respect to the major axis symmetry plane. In the solution process, the cross-section of the body and the angle of attack are modified "step-by-step" and the exact solution is obtained by the stationing principle along the coordinate x. The mesh grids are also modified in this solution process and clustered near the minor radius of the curvature.

The surface of the non-conical bodies near the vertex is assumed to be conical. At first the flow field around this cone was obtained and then, the initial data were used in computing the flow for a non-conical body.

Some results of the calculation [2] of the supersonic flow field around elliptic cones are shown in Figs. 1 and 2, and the results around a non-conical body such as a delta plane vehicle are shown in Figs. 3 and 4. The pressure p in these figures and everywhere is made dimensionless with respect to the free stream pressure p_∞ and the velocity — with to

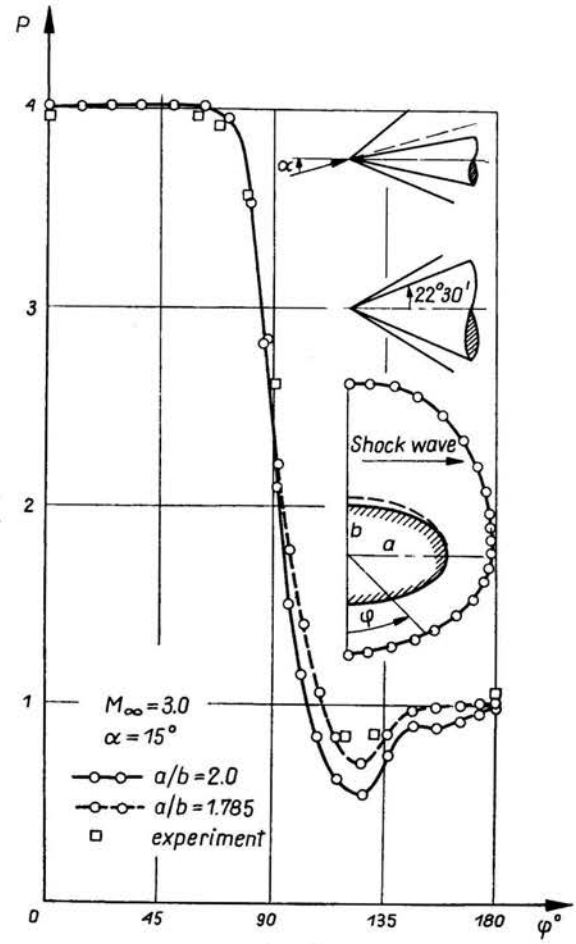

FIG. 1.

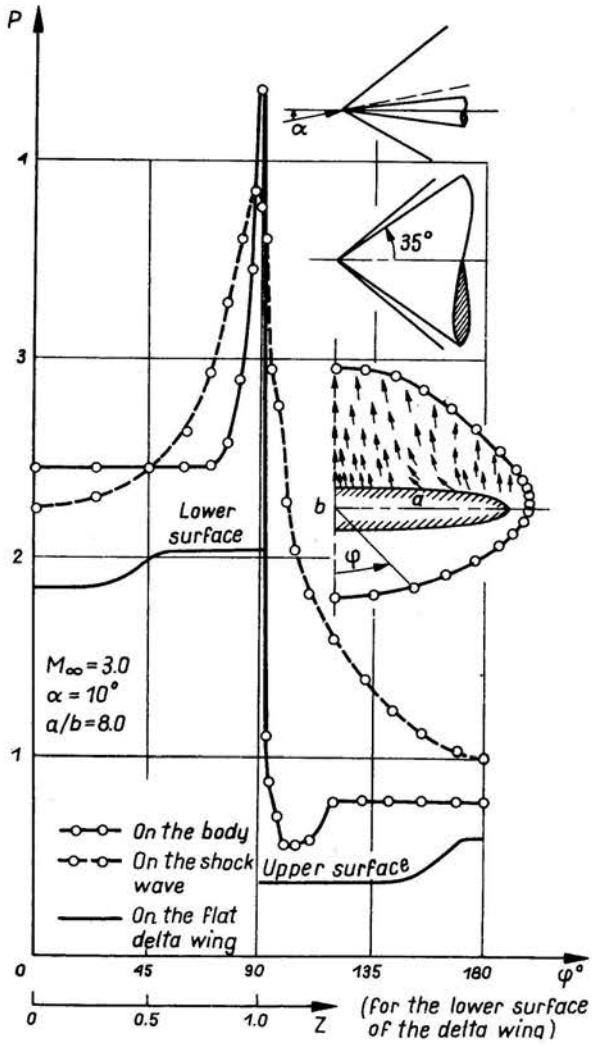

FIG. 2.

$\sqrt{p_\infty/\varrho_\infty}$, where ϱ_∞ is the free stream density. The linear dimensions of the bodies are made dimensionless with respect to their length. The pressure on the surface of the elliptic cone as a function of the meridional angle φ is shown in Fig. 1. The half-angle of the cone with respect to the major semi-axis symmetry plane is 22°30′, the ratio of the semi-axis of the cross-section ellipse $a/b = 2.0$, $M_\infty = 3.0$ and the angle of attack $\alpha = 15°$. The cross-section of the shock wave surface is also shown here. The points on this curve are mesh grid points. The pressure on the surface of the same cone obtained experimentally [3] is shown by minor squares.

On the lower, windward side of the cone, experimental pressure agrees exactly with the computed one. On the upper, leeward side we do not obtain such good agreement between numerical and experimental pressure. Experimental pressure is higher. This

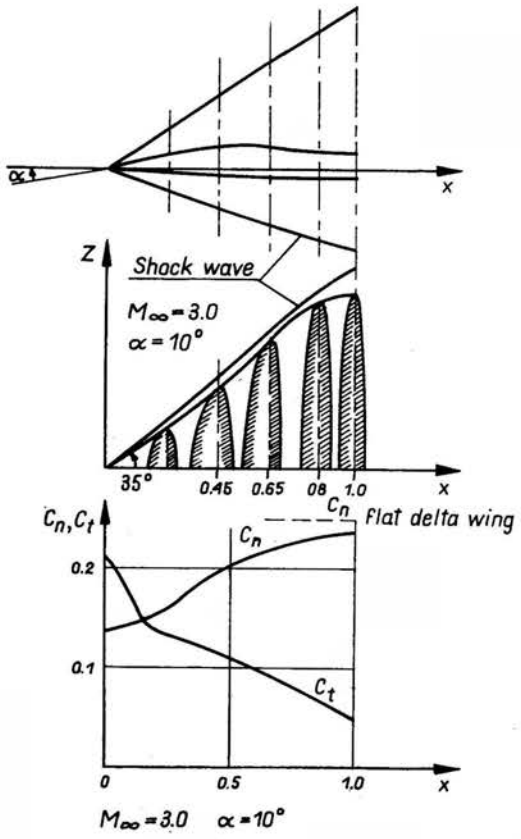

FIG. 3.

higher pressure indicates, it seems, an apparent thickening of the body in this region due to boundary-layer displacement effects. A certain numerical experiment was made to estimate this effect. The real "thickness" of the upper part of the cone is increased ($a/b = 1.78$) by the "displacement thickness" of the boundary layer on the cone. This causes the increase of the pressure on the upper side of the cone and leads to better agreement with the experiment.

Figure 2 illustrates the results of the calculation of the flow around an elliptic cone with a large ratio of the semi-axis $a/b = 8$. The half-angle of the cone with respect to the major semi-axis is 35°. The pressure distribution is shown on the cone surface and behind the shock wave. The highest pressure gradients are in those places where the curvature of the cross-section is large. Also are shown: the shock wave (the circles on the curve correspond to the mesh grid points) and the projection of the velocity vector on the $X = \text{const}$ plane for the upper side of the cone.

The pressure along the wing span on the lower and upper surfaces of the flat delta wing (from the paper [4]) is given for comparison. The shock wave is attached to the leading edge of this wing, but M_∞ and the angle of attack are the same, as those of the cone. It can

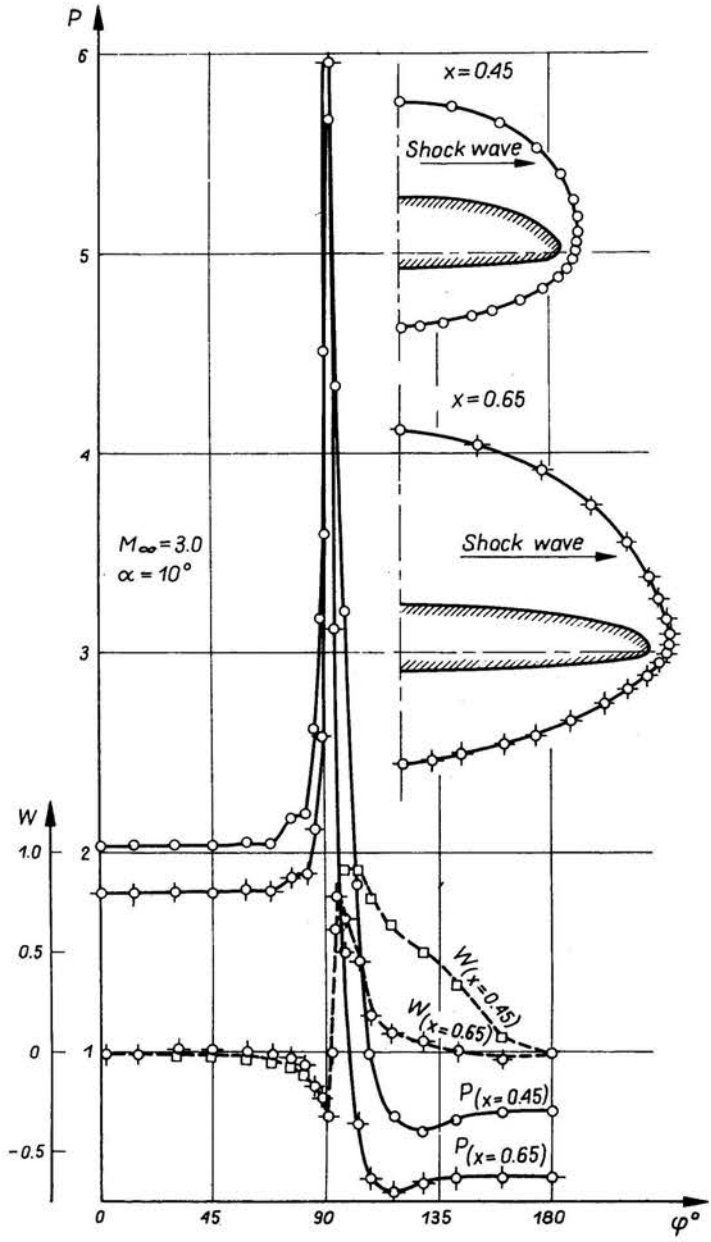

FIG. 4.

be seen that the pressure on the lower and upper halves of the cone with a large ratio of the semi-axis approaches the pressure on the delta wing.

The characteristics and the flow around a non-conical flattened body of the delta plane type are shown in Figs. 3 and 4. The cross-section of the body are different ellipses in the upper and lower halves. The shock wave, as well as the coefficients C_n and C_t, as the

functions of the coordinate x, are shown. C_n and C_t are coefficients of the normal and tangent forces. The coefficient C_n for a similar flat delta wing is given there too, to which C_n of the body is approaching.

The pressure and circular velocity component w on the surface of the body in its two cross-sections $x = 0.45$; $x = 0.65$ and also the shock wave are shown in Fig. 4. The computational points are indicated by circles. There are high pressure gradients in places where the curvature of the body cross-section is large.

3.

The second problem is concerned with the supersonic flow field around delta, swept and rhombic-shaped sharp tip wings. The wing airfoils may be arbitrary and the shock wave is attached to the leading edge of the wings. The algorithm of the lution of this problem is described in the papers [4–7]. Here we shall deal with some calculation results [7].

The Cartesian coordinates (x, y, z) are used. The domain of the solution is transformed into a rectangle by introducing the auxiliary variables

$$t = x, \quad \xi = \frac{y-G}{F-G}, \quad \theta = \frac{z}{H(t)}.$$

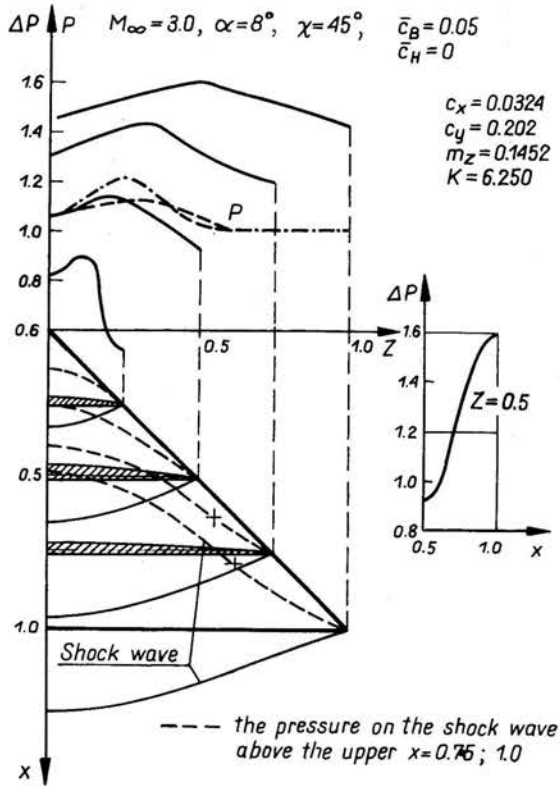

FIG. 5.

The surface of the wings is represented by the function $G = G(x, z)$, the shock wave — $F = F(x, z)$, and the leading edge of the wings — $H = H(t)$.

The initial data both on the upper and lower sides of the wings were received on the assumption that the nose of the wing is conical. The flow around the nose of the wing is determined by the stationing principle along the auto-modelling coordinate x.

The upper and lower surfaces of the wing were governed by the equation

$$y = G(t, \theta) = 4\bar{C}_{H,B}(1-\theta^{1+b})t^{1+a}[1-t-(1-\theta^{1+e})\mu(t)],$$

where

$$a = \frac{t_0}{1-t_0}, \quad \mu(t) = \left(\frac{t-t_0}{1-\mu_0-t_0}\right)^{1+d},$$

t_0 — the length of the conical nose, the coefficients: $b = 0.5$, $e = d = 0.25$, $\bar{C}_{H,B}$ — relative thickness of the airfoils, the indexes H and B correspond to the lower and upper surfaces of the wing. With $\mu_0 = 0$ is the delta wing, $\mu_0 > 0$ is the swept wing, $\mu_0 < 0$ is the rhombic-shaped wing.

In Fig. 5 calculation results of the supersonic flow around the delta wing are given. $M_\infty = 3.0$, $\alpha = 8°$, angle of sweep $\chi = 45°$ and the airfoil is flat-convex with $\bar{C}_B = 0.05$, $\bar{C}_H = 0$. The shape of the wing in the plane $y = 0$, the cross-sections of the wing and the shape of the shock wave are shown in this figure.

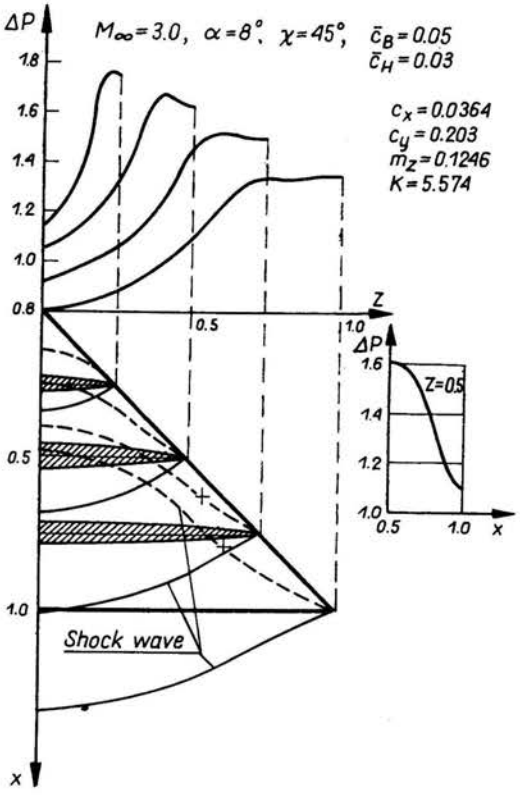

FIG. 6.

The distribution of the aerodynamical loading $\Delta p = p_l - p_u$ (where p_l — the pressure on the lower surface and p_u — the pressure on the upper surface) along the coordinate z for each cross-section, including the trailing edge, is given. The pressure behind the shock wave for the upper surface is given there too. This pressure in some region is equal to the pressure in the free stream. Here the outer shock wave is transformed into the outer characteristic surface and at the end of the wing near the leading edge there is an expansion region. That transition is shown with the crosses on the shock wave.

The character of the supersonic flow for flat wings depends on the angle of attack only and as soon as the angle of attack is positive and not equal to zero, there is an expansion region above the upper surface of the wing. But for the wings with airfoils the flow is determined not only by the angle of attack, but also by the incidence of the tangent plane to the surface of the wing. That is why at the given angle of attack, depending on the airfoil, there may be both compression and expansion flows above the wing. Besides, there may be transition from the compression region to the expansion region, as in Fig. 5. In the examples given below it takes place as well.

The loading distribution Δp along the chord of the wing at $z = 0.5$ is shown in the small plot. Here the loading along the chord increases. In Fig. 6 the results of the calculation of the flow around the wing of the same type but with the biconvex airfoil at $\bar{C}_H = 0.03$

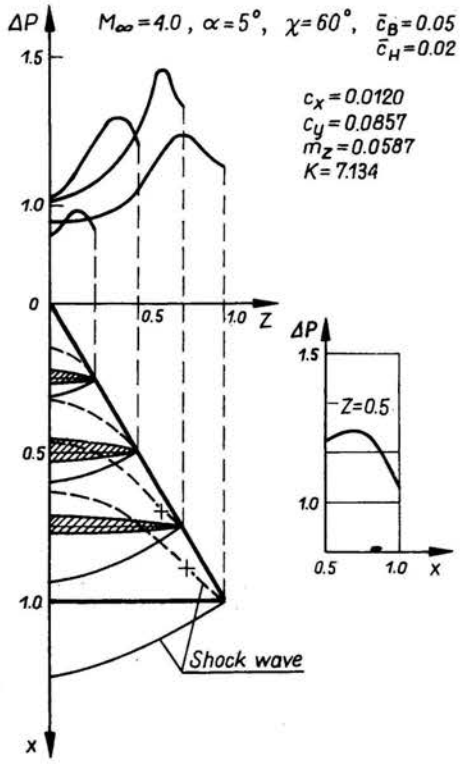

FIG. 7.

and $\bar{C}_B = 0.05$ are shown. The loading distribution is given along the span and the chord of the wing at $z = 0.5$. Here the loading along the chord drops.

The character of the loading distribution Δp along the chord for the wing with flat-convex airfoil differs from the one for the wing with biconvex airfoil. This difference, it seems, cannot be explained by the influence of the curve of the midsurface only. For example, the wing with the flat-convex airfoil at $\bar{C}_B = 0.02$ has in the plane of symmetry the same increase Δp along the chord as in Fig. 5, while the wing with the biconvex airfoil in Fig. 6 and the same curve of the midsurface has the decrease of Δp along the chord.

From here it follows, that in the loading distribution the behaviour of the upper and, particularly, lower surfaces plays a great role. Therefore, the conclusions concerning the aerodynamical characteristics of the delta wings at $M_\infty > 1$ made only on the basis of the behaviour of the midsurface may be groundless.

Figure 7 shows the same characteristics as those in Figs. 5 and 6 but for the delta wing with the sweep angle $\chi = 60°$ and Figs. 8 and 9 — for the swept and rhombic-shaped

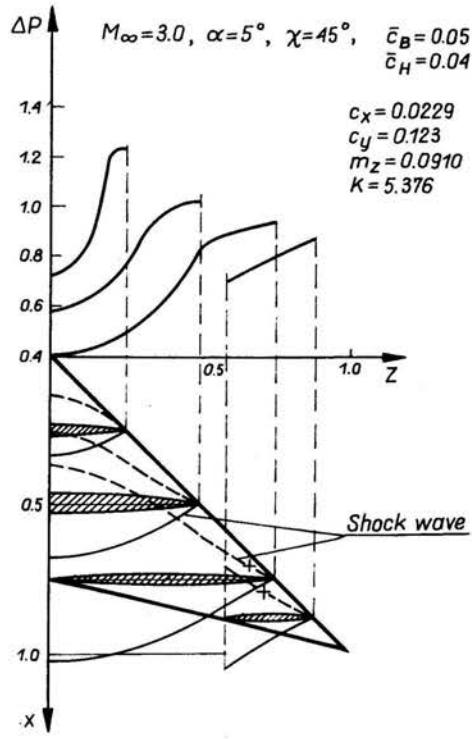

FIG. 8.

wings with biconvex airfoil. Here, the transition of the shock wave into the characteristic surface is indicated with the crosses on the shock wave.

In all figures the aerodynamical coefficients of the wings C_x, C_y, m_z in velocity coordinate systems and the aerodynamical coefficient $K = C_y/C_x$ are shown.

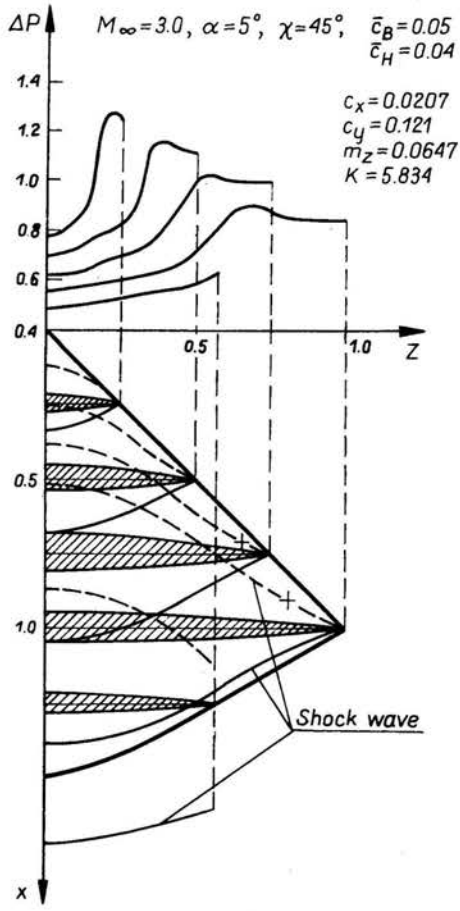

FIG. 9.

Acknowledgement

The author is grateful to V. S. TATARENCHIK, A. S. ILJINA and O. A. SHEPETIEVSKY who participated in this work.

References

1. K. I. BABENKO, G. P. VOSKRESENSKY, *Numerical method of solution for supersonic three-dimensional flow around bodies*, J. Vyčisl. Mat. i Mat.-Fiz., 6, 1961.
2. G. P. VOSKRESENSKY, V. S. TATARENCHIK, O. A. SHEPETIEVSKY, *A supersonic flow around sharp-nosed and flattened bodies*, Preprint, Inst. Appl. Math. Acad. Sci., 16, 1976.
3. A. I. SHVETS, *An investigation of the flow around elliptical cones*, Izv. AN SSSR, Mechanika židkosti i gaza, 1, 1966.
4. G. P. VOSKRESENSKY, A. S. ILJINA, V. S. TATARENCHIK, *A supersonic flow around wings with the attached shock wave*, Trudy TSAGI, 1590, 1974.

5. G. P. VOSKRESENSKY, *Numerical solution for the flow past an arbitrary surface of a delta wing in the compression region*, Izv. AN SSSR, Mechanika židkosti i gaza, 4, 1968.
6. G. P. VOSKRESENSKY, *Numerical solution for the flow past upper surface of a delta wing in expansion region*, Prikl. Mech. i Teor. Fiz., 6, 1973.
7. G. P. VOSKRESENSKY, A. S. ILJINA, V. S. TATARENCHIK, *A supersonic flow field around wings*, Preprint, Inst. Appl. Math. Acad. Sci., 104, 1976.

INSTITUTE OF APPLIED MATHEMATICS
ACADEMY OF SCIENCES, MOSCOW, USSR.

Received September 27, 1977.